

✓
KEK Proceedings 2013-9
January 2014

RADIATION DETECTORS AND THEIR USES

Proceedings of the 27th Workshop
on Radiation Detectors and Their Uses

February 5-7, 2013
High Energy Accelerator Research Organization (KEK),
Tsukuba, Ibaraki
JAPAN

Edited by
S. Sasaki, Y. Kishimoto, M. Hagiwara, T. Sanami
K. Saito, K. Iijima and H. Tawara
High Energy Accelerator Research Organization

FOREWORD

The 27th workshop on "Radiation Detectors and Their Uses" was held on February 5, 6 and 7, 2013 at the High Energy Accelerator Research Organization (KEK) in Tsukuba, Ibaraki, Japan. The workshop was hosted by the Radiation Science Center, KEK under the cooperation of the Society of Radiation Science, the affiliate of Japan Society of Applied Physics, and the Technical Committee related to Nuclear Energy of the Institute of Electrical Engineers of Japan (IEEJ). The workshop offers an outstanding opportunity for scientists interested in the fields of radiation physics, radiation detector, radiation measurement, nuclear science, high energy physics and their application to meet and discuss with colleagues from all over the country.

The number of the participants who registered to the workshop was 105. 43 presentations were given at the workshop. As the fruits of the workshop, this report was published as the proceedings of "the 27th Workshop on Radiation Detectors and Their Uses". All papers submitted for publication in the proceedings received the peer review process by the independent reviewers. Finally, 17 original papers were published in the proceedings after the review process.

The editors would like to express our great appreciation to the authors who prepared the manuscripts in good earnest and the reviewers who spent their precious time to check the papers.

November, 2013

Shinichi Sasaki

Workshop Program Chair

High energy Accelerator Research Organization (KEK)

TABLE OF CONTENTS

INFLUENCE ON CRYSTAL IDENTIFICATION PERFORMANCE OF THE 4-LAYER DOI PET DETECTOR BY MISALIGNMENT POSITION OF THE DOI BLOCK	1
<i>M. Nitta, H. Kawai, N. Inadama, F. Nishikido, Y. Hirano, E. Yoshida, H. Tashima, H. ITO, T. Yamaya</i>	
PROTOTYPE X-RAY DETECTOR OF REAL-TIME MONITORING SYSTEM FOR INTERVENTIONAL RADIOLOGY USING PLASTIC SCINTILLATORS AND OPTICAL FIBER	12
<i>F. Nishikido, H. Ito, T. Yamaya, T. Moritake, S. Kishimoto</i>	
STUDY ON SENSITIVITY OF A RADIATION DOSIMETER MADE OF A SMALL AND HEAVY PHOSPHOR IN A PHANTOM	21
<i>S. Ozaki, H. Miyamae, K. Watanabe, A. Yamazaki, A. Uritani</i>	
RESPONSE EVALUATION OF A SMALL SIZE DOSIMETER USING AN OPTICAL FIBER CONNECTING A PHOTOSTIMULABLE PHOSPHOR TO HEAVY ION IRRADIATION	25
<i>H. Miyamae, K. Watanabe, A. Uritani, A. Yamazaki, N. Matsufuji, Y. Koba</i>	
STUDY ON GLASS GEM	30
<i>T. Fujiwara, M. Uesaka, Y. Mitsuya, H. Takahashi</i>	
THE NOVEL CRYSTAL MEASURED WITH A SI-PM	38
<i>S. Kurosawa, A. Suzuki, T. Shishido, T. Sugawara, K. Yubuta, Y. Yokota, A. Yoshikawa</i>	
GROWTH OF Nd:Ca₃(Nb, Ga)₅O₁₂ SINGLE CRYSTAL AND ITS LUMINESCENT PROPERTIES	45
<i>A. Yamaji, S. Kurosawa, A. Suzuki, M. Seki, Y. Fujimoto, Y. Yokota, S. Nagata, T. Shikama, A. Yoshikawa</i>	
OBSERVATION OF THE PULSE-SHAPE PROPERTY OF A POLYETHYLENE-LINED PROPORTIONAL COUNTER FOR FAST NEUTRONS AND GAMMA-RAYS	51
<i>A. Nohtomi, F. Toyofuku, A. Sato, S. Nagamine, G. Wakabayashi</i>	
SPECTROSCOPIC MEASUREMENT OF L X-RAYS EMITTED BY TRANSURANIUM ELEMENTS BY TES MICROCALORIMETER	63
<i>M. Maeda, K. Maehata, N. Iyomoto, K. Ishibashi, K. Takasaki, K. Nakamura, K. Aoki, K. Mitsuda, K. Tanaka</i>	
DESIGN AND FABRICATION OF THE MULTI-PIXEL TES MICROCALORIMETER WITH A MUSHROOM SHAPED ABSORBER FOR X-RAY DETECTION	72
<i>S. Ezaki, K. Maehata, N. Iyomoto, S. Matsumura, K. Nagayoshi, K. Mitsuda, N. Yamasaki, Y. Takei, T. Hara, K. Tanaka</i>	
DEVELOPMENT OF TIN ABSORBER COUPLED TRANSITION EDGE SENSOR GAMMA-RAY MICROCALORIMETER	81
<i>S. Hatakeyama, M. Ohno, R. M. T. Damayanthi, H. Takahashi, Y. Kuno, C. Otani, K. Takasaki</i>	

STUDY OF RADIOACTIVITY ANALYSIS METHOD USING A THALLIUM DOPED SODIUM IODINE SCINTILLATOR WITH UNFOLDING TECHNIQUE 90
<i>M. Hayashi, T. Azuma, H. Nishizawa, H. Nakajima, S. Takushima, K. Inomata, M. Nakanishi, T. Kin, Y. Watanabe</i>	
MONTE CARLO SIMULATION OF LARGE SOLID ANGLE BETA AND GAMMA RAY DETECTORS FOR ABSOLUTE RADIOACTIVITY MEASUREMENTS 100
<i>Y. Urno, T. Sanami, M. Hagiwara, S. Sasaki, A. Yunoki</i>	
AN IDEA OF SMALL FOOD MONITOR TO DETECT RADIOCAESIUM 111
<i>Y. Ogata</i>	
DEVELOPMENT OF ON-LINE C₆₀-60 MONITORING SYSTEM FOR PRIMARY COOLANT PIPES IN PRIMARY CONTAINMENT VESSEL OF NUCLEAR POWER PLANTS 118
<i>K. Ueno, T. Tadokoro, M. Tsuyuki, H. Matsubara, N. Ota, M. Nagase</i>	
EVALUATION AND CALCULATION OF PERTURBATION CORRECTION FACTORS FOR IONIZATION CHAMBER IN RADIOTHERAPY WITH MONTE CARLO SIMULATION CODES EGS5/PHITS 128
<i>M. Matsumoto, Ken Shiozaki, M. Takashina</i>	
MEASUREMENT OF SPACE CHARGE FROM A PRINTED CIRCUIT BOARD IRRADIATED WITH LOW-LEVEL GAMMA-RAYS 138
<i>H. Ichiki, H. Higaki, M. Ogata, T. Matsuoka, Y. Hirayama, T. Furuzumi, K. Futagami, T. Kawaguchi</i>	

AN OBSERVATION OF THE PULSE-SHAPE PROPERTY OF A POLYETHYLENE-LINED PROPORTIONAL COUNTER FOR FAST NEUTRONS AND GAMMA-RAYS

Akihiro Nohtomi* and Fukai Toyofuku
Department of Health Sciences, Faculty of Medical Sciences, Kyushu University
3-1-1 Maidashi, Higashi-ku, Fukuoka 812-8582, JAPAN

Ayaka Sato
Department of Health Sciences, School of Medicine, Kyushu University
3-1-1 Maidashi, Higashi-ku, Fukuoka 812-8582, JAPAN

Syuji Nagamine
Department of Radiology, Kyushu University Hospital
3-1-1 Maidashi, Higashi-ku, Fukuoka 812-8582, JAPAN

Genichiro Wakabayashi
Atomic Energy Research Institute, Kinki University
3-4-1 Kowakae, Higashi-Osaka-shi, Osaka 577-8502, JAPAN

1. INTRODUCTION

We have been doing basic investigations with aiming at the development of a fast-neutron survey meter, which is simple, practical and user-friendly such as a GM tube for photons. Our interest is mainly centered on the neutrons from 100 keV to 10 MeV because the values of the neutron radiation-weighting factor exceed 10 in the energy region. Therefore, a daily quick check of such fast neutrons is very favorable for the radiation protection aspects in various situations including recent medical fields, such as those of high energy X-ray radiotherapy.

At present, a rem counter is commonly used in medical facilities to survey neutron dose-equivalent [Sv]. A rem counter is usable for a wide energy range of neutrons from thermal neutron region up to a few tens of MeV one. On the other hand, when focusing on the fast neutron detection only, another possible candidate is a recoil-proton proportional counter. Especially, converter-lined type counters, such as a polyethylene-lined proportional counter, seem to have an advantage in the detection efficiency because they have high conversion probabilities superior to those of gas-conversion type counters (or gas recoil counters) owing to the high atomic density of hydrogen in a solid material. When such recoil-proton

* *Corresponding author*, (tel)092-642-6722, (fax)092-642-6723, (e-mail)nohtomi@hs.med.kyushu-u.ac.jp

proportional counters are applied for fast neutron measurements, the most critical issue to be solved is an elimination of gamma-rays. So far, no commonly available means has been established for the discrimination of fast neutron signals from gamma signals by recoil-proton proportional counters; a simple discrimination solely by amplitude does not work well often. In this paper, from the view points mentioned above, pulse shapes produced by a polyethylene-lined recoil-proton proportional counter, LND 28220, have been studied by both a digital method and an analogue method with various neutron sources.

2. POLYETHYLENE-LINED PROPORTIONAL COUNTER

The counter used in the present study is a polyethylene-lined proportional counter (LND 28220, S.N. 382604) that is a modified version of the LND 2823 [Fig.1]. The original gas filling (P-10 gas in 432 Torr) has been changed to sole CH_4 in 760 Torr (101.3 kPa)⁽¹⁾ because reliable experimental data of electron drift velocity in CH_4 are available for the calculation of output pulse shape. The cathode wall is made of a stainless-steel pipe whose outer diameter is 25.4 mm and the inner diameter 24.4 mm. An anode wire (50.8 μm in diameter) is stretched along the axis to have an effective counter length of 213.4 mm. The inner surface of the cathode is lined with a 1.5 mm-thick polyethylene layer as a converter. The converter is properly conditioned by manufacturer so as not to have surface-charge accumulations.

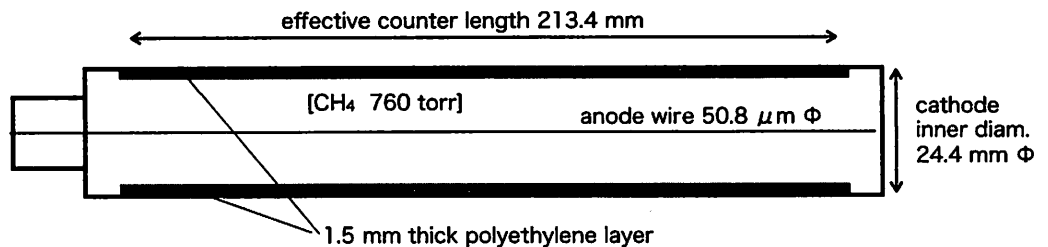


Fig. 1. LND 28220 polyethylene-lined proportional counter.

For gas-conversion type counters, such as a hydrogen-filled proportional counter, the difference of ionization track lengths in neutron and gamma events has been conventionally utilized for their discrimination⁽²⁾. The long electron track in a gamma event causes a relatively long rise-time (typically a few micro seconds). On the other hand, the short proton track in a neutron event gives a rather shorter rise-time of around a microsecond or less. A typical example of such discrimination based on the difference of rise-time information is given in Fig. 2⁽³⁾. This rise-time discrimination, or pulse-shape discrimination, is usually applicable to low energy neutrons only, because the long proton tracks created by high energy neutrons are not distinguishable from electron tracks in the rise-time information. Therefore, it should be kept in mind that the conventional method cannot be applied to the present measurement of fast neutrons from such a theoretical background, primarily.

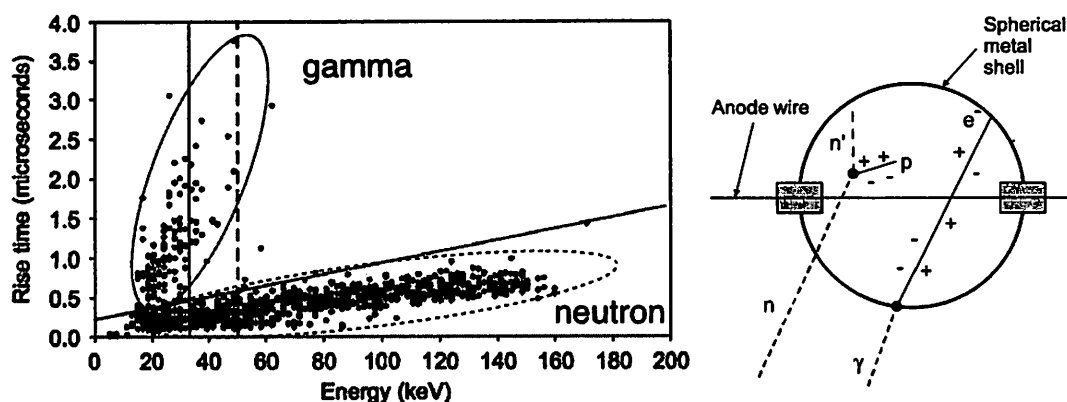


Fig. 2. An example of two-dimensional plots of the rise-time and the pulse amplitude (energy) obtained from the 3-atm SP2 counter exposed to 144 keV neutrons ⁽³⁾.

3. EXPERIMENTAL

The pulse-shape observation was carried out in a low-scatter room at the National Physical Laboratory (NPL) in the United Kingdom using a variety of neutron sources: ²⁵²Cf, ²⁴¹Am-Be, ²⁴¹Am-B, ²⁴¹Am-F and ²⁴¹Am-Li ⁽⁴⁾. Excepting the ²⁵²Cf, these neutron sources were commonly set with a 6.6 mm-thick lead cap in order to reduce the gamma-ray intensity. A ¹³⁷Cs source was also used to check the response to pure gamma-rays. The counter was arranged close to the middle of the low-scatter room. The cylindrical-shape sources were put near the counter; the distance between counter-axis and source-axis was fixed to be 83 mm for all measurements.

Fig. 3 shows a diagram of the electronics used in this experiment. The pulses from the counter (LND 18220) were fed into a charge sensitive preamplifier (OKEN 703-1C). For the digital method, the output of preamplifier was connected to a timing amplifier (ORTEC 574) followed by a 12-bit high speed digitizer (Agilent U1070A Acqiris DP310, 400 MS/s) which was inserted to a PCI slot of a control PC; data acquisition and analysis were also done by using this PC. For the analogue method, the output of the preamplifier was sent to a spectroscopy amplifier (ORTEC 572). After a shaping with the time constant of 1 μ s, the unipolar output was connected to a rise-time to height converter (OKEN 723-1C) for the rise-time measurement, or to a pulse shape analyzer (ORTEC 552) combined with a time to amplitude converter (ORTEC 457) for the fall time measurement. Two constant-fraction discriminations of the pulse-shape analysis were set to 10% and 90% commonly for both rise-time and fall-time measurements; the same settings of discrimination levels were also used for the off-line analysis by the digital method. Resultant pulse heights of the analogue method were recorded by a multi-channel analyzer system (ORTEC Easy-MCA). Above three pulse-shape analyses were carried out in order to confirm the consistency of the observations of an identical phenomenon by different means.

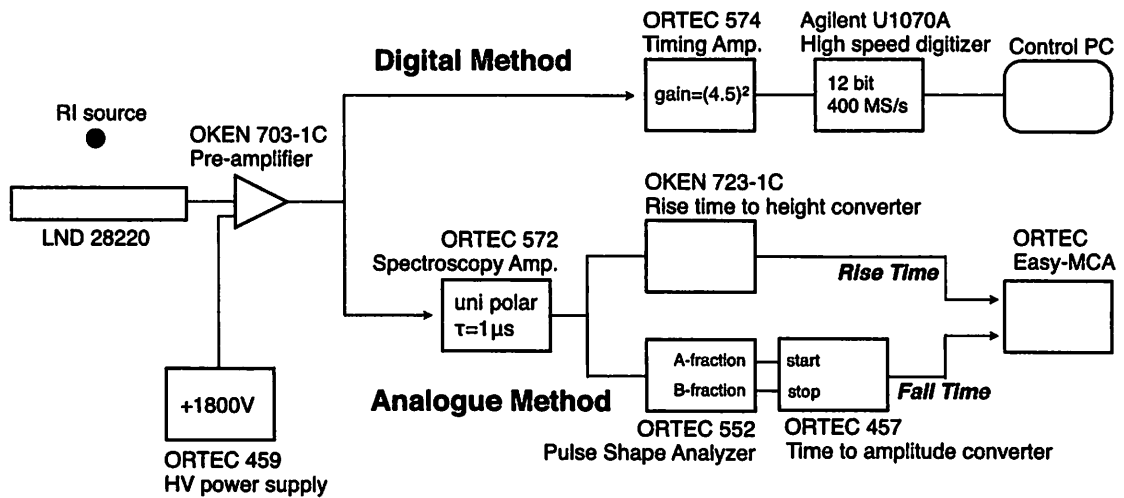


Fig. 3. Diagram of electronics used in the experiment.

4. RESULTS AND DISCUSSION

4.1 Rise-time distributions by the digital method

Fig. 4 (a) shows the rise-time (10% - 90%) distributions obtained by the digital method for $^{241}\text{Am-Be}$, $^{241}\text{Am-B}$, $^{241}\text{Am-Li}$ and ^{252}Cf sources. About 5000 events were recorded for each measurement. The vertical axis was normalized by the number of total events. Two separate distributions are clearly noticeable in the figure. One has a peak at about $0.5\ \mu\text{s}$ with ranging from around $0.3\ \mu\text{s}$ to $0.8\ \mu\text{s}$ (referred as “Peak-A” hereafter). The other has a peak at about $1.6\ \mu\text{s}$ with ranging from around $1.4\ \mu\text{s}$ to $3\ \mu\text{s}$ (referred as “Peak-B” hereafter). When the ^{137}Cs gamma-ray source ($0.662\ \text{MeV}$) was put, Peak-B disappeared and only Peak-A remained as shown in Fig. 4 (b); about 1000 events were recorded for the ^{137}Cs measurement and the vertical axis was normalized by the number of total events. From these observations, we can straightforwardly say that Peak-A corresponds to gamma events and Peak-B corresponds to neutron events. Low energy gamma events from ^{241}Am (dominant energy $\sim 60\ \text{keV}$) were efficiently reduced by the 6.6-mm thick lead shielding. Gamma events from ^{252}Cf were also not so much because the radio activity of ^{252}Cf is relatively far smaller ($0.121\ \text{MBq}$) in comparison with the activity of other ^{241}Am sources ($185\ \text{GBq}$ for $^{241}\text{Am-Li}$, $37\ \text{GBq}$ for $^{241}\text{Am-B}$ and $^{241}\text{Am-Be}$). In addition to these gamma-rays, the $^{241}\text{Am-Li}$ source emits rather high energy gamma-rays (dominant energy $\sim 0.478\ \text{MeV}$) through $^7\text{Li}(\alpha, \alpha' \gamma)^7\text{Li}$ reaction⁽⁵⁾ and the 6.6-mm thick lead was not sufficient for shielding these gamma-rays. The significant contribution of such a gamma event is evident in Fig. 4 (a).

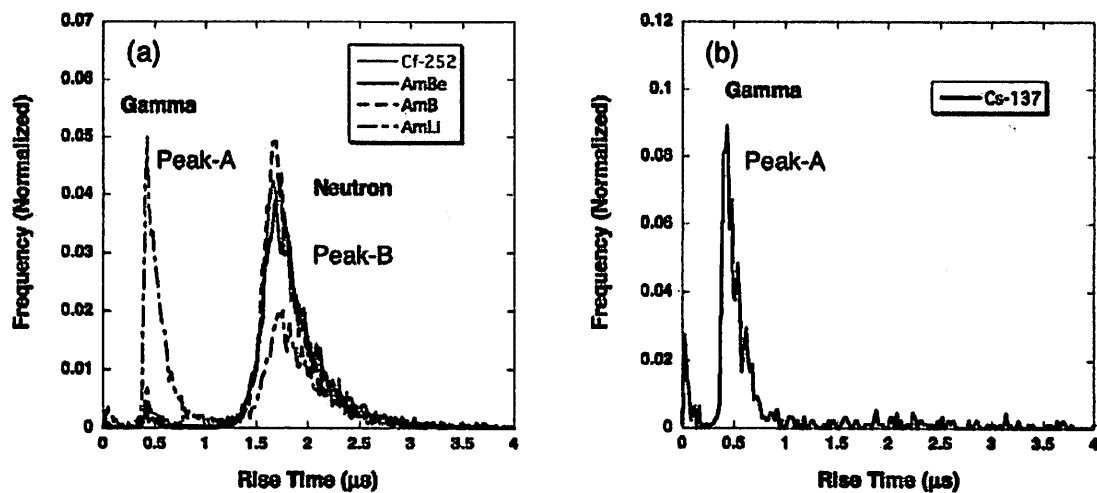


Fig. 4. Rise-time (10%-90%) distributions obtained by the digital method.

The data in Fig. 4 are reproduced in a two-dimensional form of the rise-time and the amplitude for $^{241}\text{Am-Be}$, $^{241}\text{Am-Li}$, ^{252}Cf and ^{137}Cs in Fig. 5. Because the internal trigger input of the high speed digitizer accepts the amplitudes larger than about 10% of the full-scale setting, small pulses were discriminated and missing for these measurements. In those plots, neutron regions indicate a nearly triangle-like shape, which are common to $^{241}\text{Am-Be}$, $^{241}\text{Am-Li}$ and ^{252}Cf . With an increase of the rise-time from 1.4 μs to 1.6 μs , the largest values of amplitude extend up to about 0.25 V. This is related to the increase of rise-time when the track of recoil-proton becomes longer in the counter. The maximum amplitude of 0.25 V may correspond to the largest energy-loss of a recoil proton in CH_4 gas; that can be roughly calculated to be about 0.9 MeV by assuming the full-energy deposition of a proton whose range is just equivalent to the diameter of counter cross-section of gas region, 21.3 mm. In contrast with this, for the further increase of rise-time beyond 1.6 μs , the largest values of amplitude show a distinctive decrease that is approaching to the discrimination level by around 3 μs . That means such relatively long rise-time is caused by a high energy proton which penetrates the gas region and loses only a part of its energy in CH_4 . A possible explanation of this observation may be given as follows. Inevitably, such a high energy proton hits the wall and may deposit a large part of its energy there. As the result, it may be quite possible that a certain amount of electrons are emitted from the surface of polyethylene-wall by the impact of proton. Those electrons can effectively prolong the pulse rise-time because such electrons create additional ionization at the farthest place from the anode wire, and the ionization reaches to the gas-multiplication region with a relatively long delay after the arrival of ionization from the nearest part.

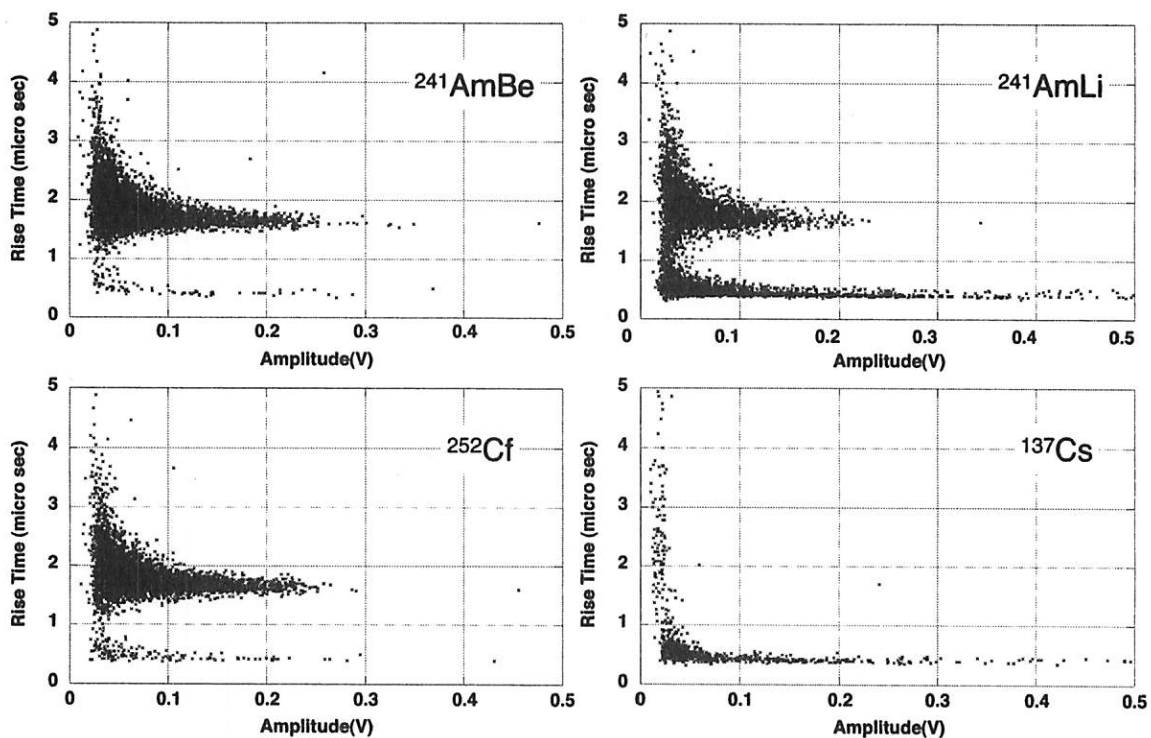


Fig. 5. Two-dimensional plots of rise-times and amplitudes by the digital method.

Regarding the gamma events, the very quick rise-time in Fig. 4 ($\sim 0.5 \mu\text{s}$) is unexpected and quite difficult to understand, in conjunction with an unusual observation in the two-dimensional plots of gamma events in Fig. 5, which is obviously different from the correlations obtained by conventional gas recoil counters in Fig. 2. Further discussion on this matter will be attempted in Section 4.3 with a calculation of output pulse shapes.

4.2 Rise-time and fall-time distributions by the analogue method

Rise-time distributions measured by the analogue method are shown in Fig. 6 (a) [for $^{241}\text{Am-Be}$] and Fig. 6 (b) [for $^{241}\text{Am-Li}$]. Fig. 6 (c) displays that of gamma-rays for ^{137}Cs together with other four gamma-ray distributions which were obtained by subtracting the rise-time distributions with the lead-cap from those without the cap for $^{241}\text{Am-Be}$, $^{241}\text{Am-B}$, $^{241}\text{Am-F}$ and $^{241}\text{Am-Li}$ sources; all distributions were normalized by the maximum values in the vertical axis. One can notice that all curves are almost identical and overlap each other. The dashed line in Fig. 6 (c) indicates a fitted curve of the average of above 5 distributions by an "Extreme function"⁽⁶⁾. Extreme function $y(x)$ is defined as follows:

$$\begin{cases} y(x) = A \exp[-\exp(-z) - z + 1] + B \\ z = \frac{x-a}{b} \end{cases} \quad (1)$$

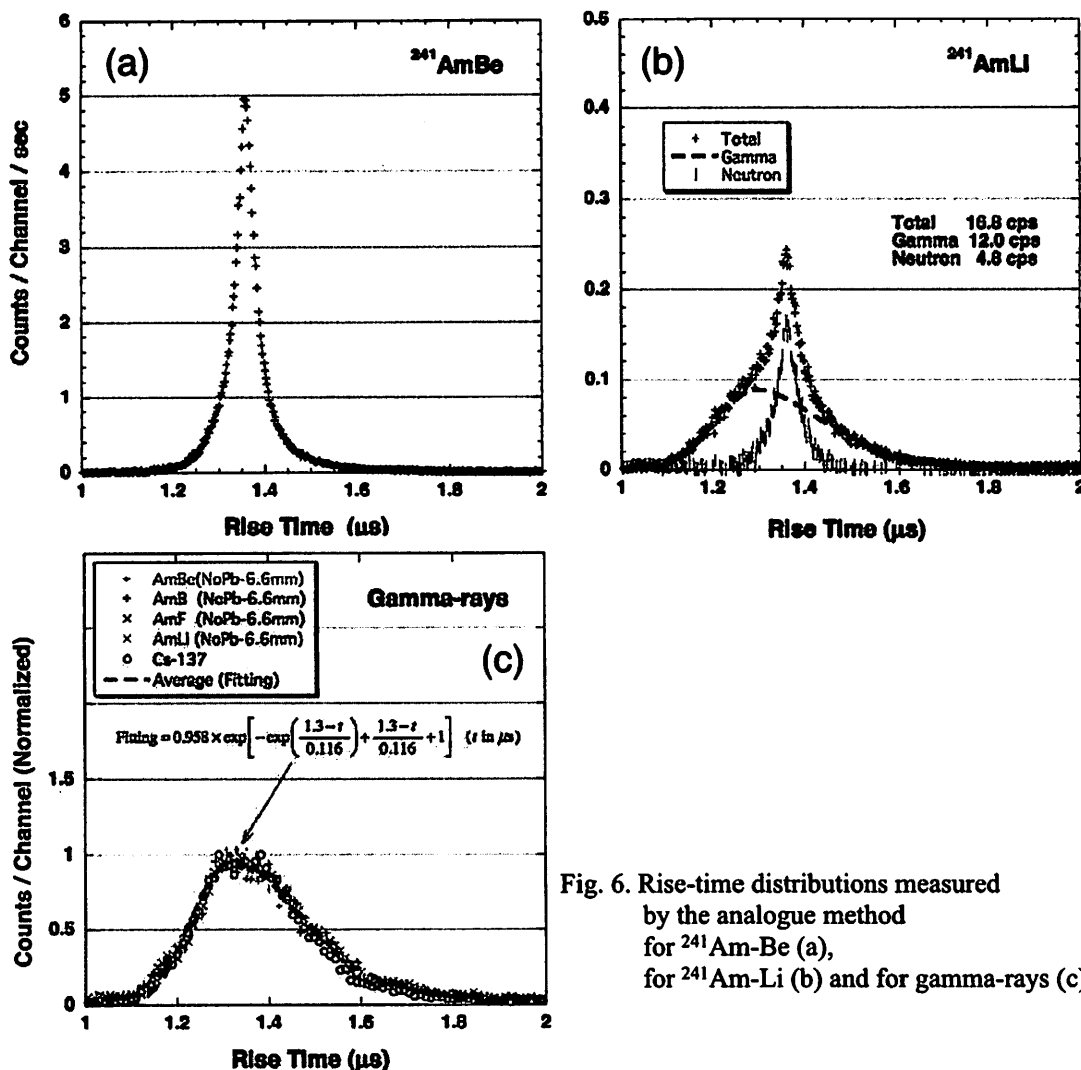


Fig. 6. Rise-time distributions measured by the analogue method for $^{241}\text{Am-Be}$ (a), for $^{241}\text{Am-Li}$ (b) and for gamma-rays (c).

In the rise-time distribution for $^{241}\text{Am-Be}$ [Fig. 6 (a)], neutron events may essentially dominate owing to very efficient shielding of gamma events by the lead-cap; the peak is located at 1.36 μs with ranging from about 1.2 μs to 1.6 μs . Similar peaks were also found in the rise-time distributions for $^{241}\text{Am-B}$ and $^{241}\text{Am-F}$. On the other hand, a significant contribution of gamma events is apparent for $^{241}\text{Am-Li}$, as shown in Fig. 6 (b). Therefore, after subtracting the corresponding neutron peak (1.2 μs ~ 1.6 μs) from it, the remained distribution was fitted by the Extreme function determined in Fig. 6 (c). By this, the neutron events and the gamma events were separated appropriately and plotted in the same figure with their count rates. The separated neutron distribution also has a peak at 1.36 μs .

Similar distributions were also observed for the fall-time measurements. The results are plotted in Fig. 7 (a) [for $^{241}\text{Am-Be}$], Fig. 7 (b) [for $^{241}\text{Am-Li}$] and Fig. 7 (c) [for gamma rays] by the same manner with the rise-time measurements. In the fall-time measurements, the neutron peak is commonly located at 3.4 μs . Because the neutron peak ranges relatively wider in comparison with the rise-time measurements, a considerable overlap with the gamma peak exists. So, in Fig. 7 (b), the separation of both peaks was carried out by carefully taking account of the consistency of their count rates with those for Fig. 6 (b).

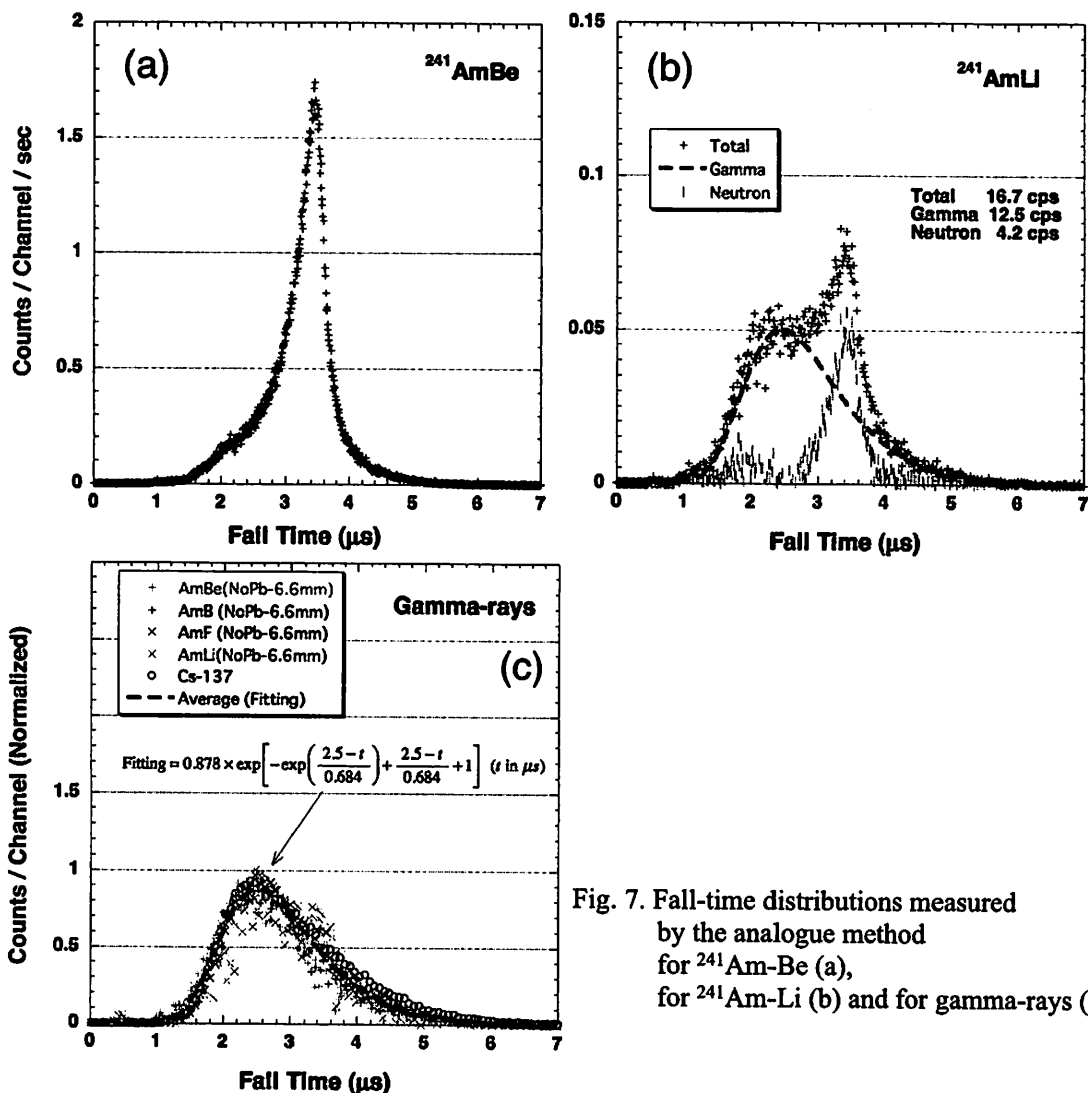


Fig. 7. Fall-time distributions measured by the analogue method for $^{241}\text{Am-Be}$ (a), for $^{241}\text{Am-Li}$ (b) and for gamma-rays (c).

From the above observations by the analogue method, we notice a remarkable separation between the neutron peak and the gamma peak still remains even after a differential pulse-shaping of $\tau = 1 \mu\text{s}$, although it is significantly blurred. The shapes of both peaks do not vary so much for various neutron sources having quite different energy spectra.

4.3 Calculation of output pulse shape

Fig. 8 indicates typical pulse shapes of neutron events (a), and gamma events (b), observed by the digital method. As shown in the figure, both are apparently distinguishable. In order to study these observations, the shapes of the output pulse for the present proportional counter were calculated on the basis of Eq. (6.37) of Ref. (7). In the calculation, the mobility of CH_4 molecular positive-ion was chosen to be $2.26 \text{ cm}^2/\text{s/V}$ at the normal condition ⁽⁸⁾. The electron drift velocity in CH_4 was obtained from the experimental data by Hunter et al. ⁽⁹⁾. A differential pulse shaping was also taken account into the calculation, which was built in the preamplifier used.

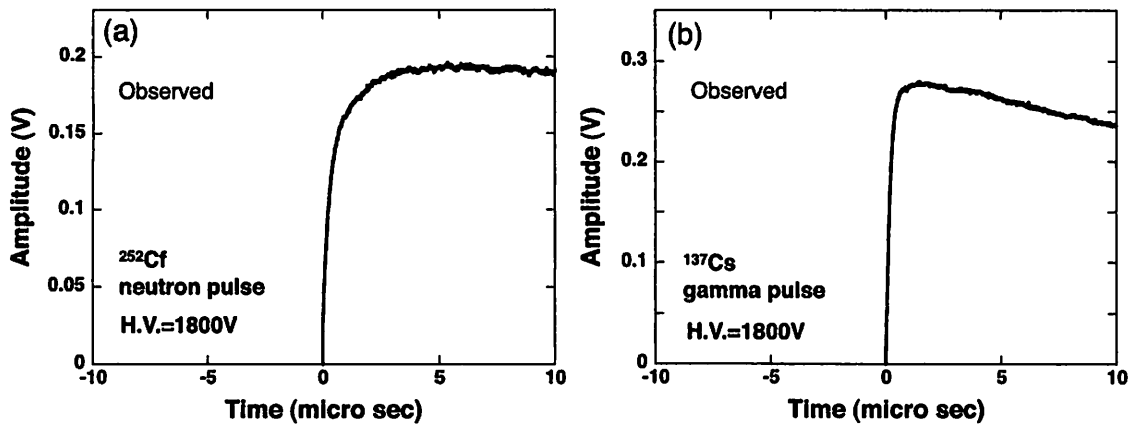


Fig. 8. Typical pulse shapes of neutron events (a) and gamma events (b) observed by the digital method.

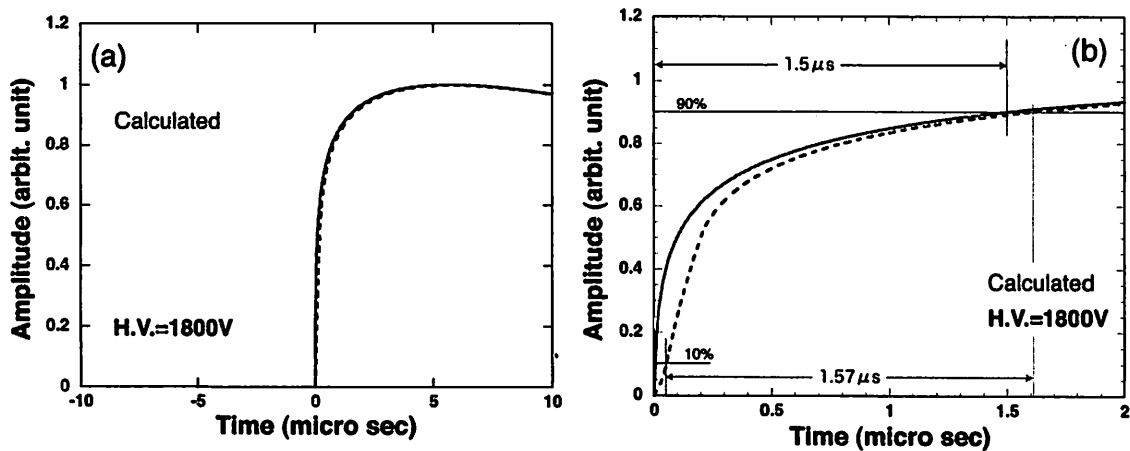


Fig. 9. Calculated results of pulse shapes. The solid line represents initial ionization formed at a single radius. The dashed line assumes a uniform ionization along the diameter.

The calculated results are shown in Fig. 9 (a), whose axis range and appearance are adjusted for a direct comparison with Fig. 8; the vertical axis is normalized by the maximum amplitude. In the figure, the solid line represents initial ionization formed at a single radius. On the other hand, the dashed line assumes a uniform ionization along the diameter. For the calculation, the time constant of a differential shaping is chosen to be $40 \mu\text{s}$ instead of the default value of $50 \mu\text{s}$ in order to reproduce experimental more adequately. Consequently, we find that the calculation in Fig. 9 (a) explains well the neutron pulse in Fig. 8 (a). A magnified view around the leading edge of the same calculation is presented in Fig. 9 (b). In the figure, 10%-90% rise-time of the solid line is $1.5 \mu\text{s}$. This value is roughly equivalent to the shortest rise-time of neutron events observed in Fig. 4, i.e. $1.4 \mu\text{s}$. That of the dashed line is $1.57 \mu\text{s}$. This may correspond to the rise-time of a neutron pulse having the largest amplitude ($\sim 0.25 \text{ V}$) in Fig. 4, i.e. $1.6 \mu\text{s}$.

From the calculated results in Fig. 9, we also notice that the pulse shape of gamma-ray event, Fig. 8 (b), is very difficult to explain properly by a conventional theory of the proportional pulse formation used

here. If the pulse originated from the normal proportional mode, the shortest rise time should be simply given by the single-radius ionization, a solid curve in Fig. 9. Therefore, a short rise-time less than $1.5 \mu\text{s}$ is out of scope. Another inexplicable observation is the large amplitudes of gamma events exceeding the maximum amplitude of neutron events. Moreover, such large pulses indicate very short rise-times as well [Fig.8 (b)]. This is contradictory to a general understanding that a large pulse of gamma-ray event is accompanied with a long electron track in a proportional counter, and then a long rise time. From these reasons, it seems that as if the gas multiplication of this detector occurs in an unusual way for gamma-ray events only.

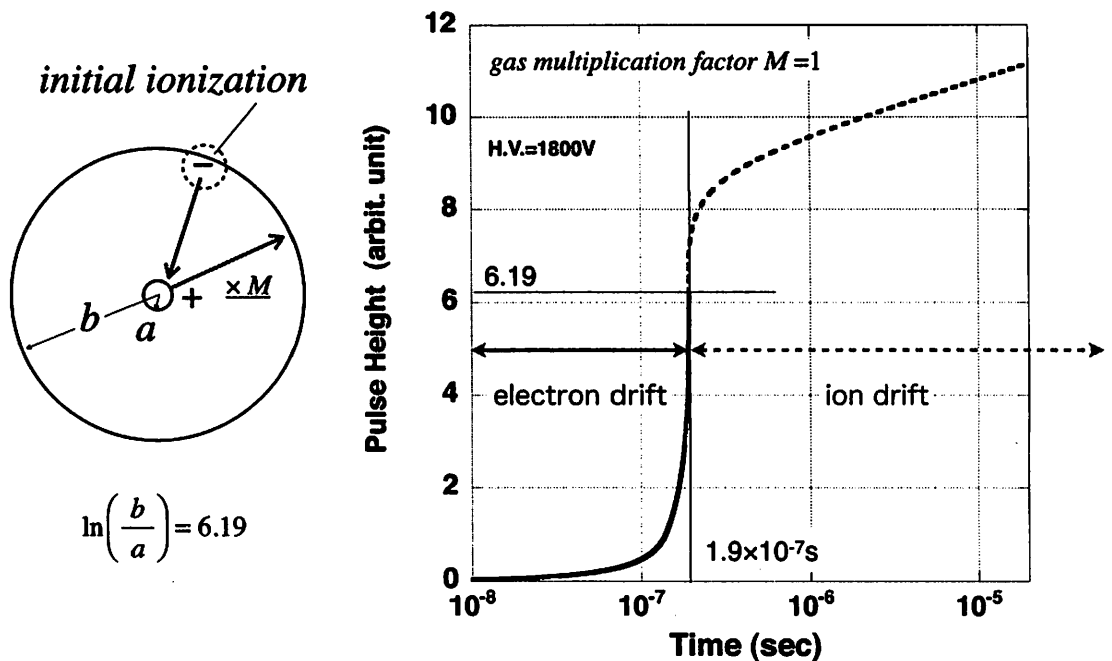


Fig. 10. A simplified model assuming the contribution of electron drift, and the calculated results.

In order to understand the curious behavior of gamma-ray events mentioned above, as an attempt, we carried out some additional calculations on the basis of a simplified model as described in Fig. 10. In the model, the contribution of electron drifting to pulse formation was tentatively assumed to be equivalent to that of ion drifting; the initial ionization was generated at the inner surface of cathode wall and the gas multiplication factor M was unity. The electron-drifting behavior was evaluated from experimental data in CH_4 by Hunter et al. ⁽⁹⁾. Then, the calculated result of Fig. 10 is reproduced in Fig. 11 for a direct comparison with observed pulses in Figs. 8. After the differential pulse shaping, we notice that the calculation explains the pulse by gamma rays in Fig. 8 (b) rather adequately.

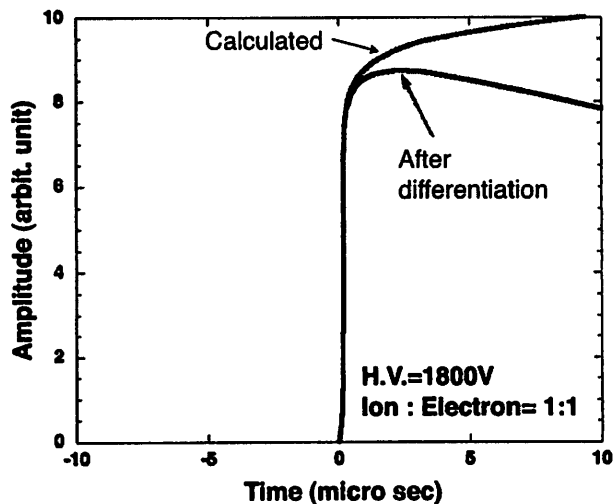


Fig. 11. Calculated pulse shape on the basis of the simplified model. The same data of Fig. 10 is reproduced in a different manner for a direct comparison with the observations in Fig. 8.

5. CONCLUSION

Output pulse shapes of a polyethylene-lined proportional counter have been studied by both a digital method and an analogue method for various neutron sources. The results suggested that the time behaviors of neutron events and gamma events were apparently different in this counter. Consequently, two kinds of pulse shapes were distinguishable each other. A clear and straightforward observation of rise time by the digital method was an evidence of this conclusion. Other measurements by the analogue method were consistent with those by the digital method and also supported such a conclusion. The experimental facts found in the present study may be very useful for the practical discrimination of fast neutrons from gamma rays. On the other hand, however, a proper interpretation of such unconventional separation has not been achieved yet. Especially, it seems likely that the very short rise time of gamma-ray events is rather hard to explain within the framework of conventional understandings on a proportional counter. A rough and tentative assumption (the contribution of electron drifting is equivalent to that of ion drifting) successfully led to a proper calculation of pulse shape for gamma-ray events. But, for such a theoretical calculation, a possible electron-feeding mechanism is lacking at the distant position from the anode. Moreover, it is unknown why a similar event does not occur for neutron events; the pulse shapes for neutrons seem to be reasonable and rather easy to be explained by the conventional theory of a proportional counter.

To get more sufficient understanding on this subject, further careful works should be done in the future. For example, the gas multiplication characteristics must be measured for gamma-rays by some means and compared with the theoretical expectations. The influence of existence of a polyethylene layer on the gas multiplication process may be also another essential subject to be examined. In addition, as a

possible explanation, an unusual but significant contribution of electrons, as well as ions, to the pulse formation should be discussed more thoroughly, including the electron-feeding mechanism.

ACKNOWLEDGEMENTS

We are grateful to Drs. D. J. Thomas, N. J. Roberts, G. C. Taylor and N. P. Hawkes of National Physical Laboratory (NPL) for their kind cooperation in the experiment. Some authors are indebted to Dr. H. Harano of NMIJ and Dr. T. Sakae of PMRC for their valuable discussions. One of the authors (A.N.) wishes to thank Mr. Y. Kawabata and Mr. D. Nakanishi of Kyushu University for their assistance to the preliminary experiments. This work was partially supported by the grant-in-aid of Educational Enhancement Program (EEP) 2011 of Kyushu University, Fukuoka, Japan.

REFERENCES

- (1) LND, INC., (Web site) <http://www.lndinc.com/>
- (2) G. F. Knoll, Radiation Detection and Measurements, fourth ed., John Wiley and Sons, Inc., New York (2010) p. 583.
- (3) N. P. Hawkes, Nucl. Instr. and Meth. A 574 (2007) p. 133.
- (4) N. P. Hawkes, Nucl. Instr. and Meth. A 580 (2007) p. 183.
- (5) C. J. McKay, P. Burgess, N. P. Hawkes, M. Kelly, G. C. Taylor and D. J. Thomas, "Photon Doses in NPL Standard Radionuclide Neutron Fields", NPL REPORT IR 12 (2009) p. 6.
- (6) Computer Program "ORIGIN 8" (OriginLab Co.), nonlinear curve fitting functions.
- (7) G. F. Knoll, Radiation Detection and Measurements, fourth ed., John Wiley and Sons, Inc., New York (2010) p. 182.
- (8) F. Sauli, "Principles of operation of multiwire proportional and drift chamber", CERN 77-09 (1977) p. 20.
- (9) S. R. Hunter, J. G. Carter and L. G. Christophorou, J. Appl. Phys. 60 (1986) p. 24.